Journal of Advanced Research 16 (2019) 43–53

Contents lists available at ScienceDirect

Journal of Advanced Research

journal homepage: www.elsevier.com/locate/jare

Original Article

NiSn nanoparticle-incorporated carbon nanofibers as efficient electrocatalysts for urea oxidation and working anodes in direct urea fuel cells

Nasser A.M. Barakat [a,*], Mohamed T. Amen [b], Fahad S. Al-Mubaddel [c], Mohammad Rezual Karim [d], Maher Alrashed [c]

[a] Chemical Engineering Department, Minia University, PO Box 61519, El-Minia, Egypt
[b] Bionano System Engineering Department, College of Engineering, Chonbuk National University, PO Box 54896, Jeonju, South Korea
[c] Department of Chemical Engineering, King Saud University, PO Box 800, Riyadh 11421, Saudi Arabia
[d] Center for Excellence in Materials Research CEREM, King Saud University, PO Box 800, Riyadh 11421, Saudi Arabia

HIGHLIGHTS

- Influence of tin as a co-catalyst for nickel toward urea oxidation is proposed.
- Tin co-catalyst shows very high current density; 175 mA/cm^2.
- The calcination temperature was optimized; 850 °C is the best.
- The corresponding onset potential is 175 mV which indicates applicability in DUFC.
- Synthesis process is effective, simple and high yield technology; electrospinning.

GRAPHICAL ABSTRACT

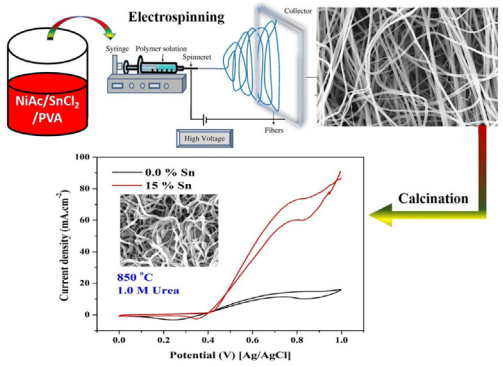

ARTICLE INFO

Article history:
Received 24 September 2018
Revised 12 December 2018
Accepted 14 December 2018
Available online 16 December 2018

Keywords:
Urea fuel cell
Urea electrolysis
NiSn carbon nanofibers
Electrospinning

ABSTRACT

Synthesis of NiSn alloy nanoparticle-incorporated carbon nanofibers was performed by calcining electrospun mats composed of nickel acetate, tin chloride and poly(vinyl alcohol) under vacuum. The electrochemical measurements indicated that utilization of tin as a co-catalyst could strongly enhance the electrocatalytic activity if its content and calcination temperature were optimized. Typically, the nanofibers prepared from calcination of an electrospun solution containing 15 wt% $SnCl_2$ at 700 °C have a current density almost 9-fold higher than that of pristine nickel-incorporated carbon nanofibers (77 and 9 mA/cm^2, respectively) at 30 °C in a 1.0 M urea solution. Furthermore, the current density increases to 175 mA/cm^2 at 55 °C for the urea oxidation reaction. Interestingly, the nanofibers prepared from a solution with 10 wt% of co-catalyst precursor show an onset potential of 175 mV (*vs.* Ag/AgCl) at 55 °C, making this proposed composite an adequate anode material for direct urea fuel cells. Optimization of the co-catalyst content to maximize the generated current density resulted in a Gaussian function peak at 15 wt%. However, studying the influence of the calcination temperature indicated that 850 °C was the optimum temperature because synthesizing the proposed nanofibers at 1000 °C led to a decrease in the graphite content, which dramatically decreased the catalyst activity. Overall, the study opens a new venue for the researchers to exploit tin as effective co-catalyst to enhance the electrocatalytic

Peer review under responsibility of Cairo University.
* Corresponding author.
E-mail address: nasbarakat@minia.edu.eg (N.A.M. Barakat).

https://doi.org/10.1016/j.jare.2018.12.003
2090-1232/

performance of the nickel-based nanostructures. Moreover, the proposed co-catalyst can be utilized with other functional electrocatalysts to improve their activity toward oxidation of different fuels.

Introduction

Due to its relatively high hydrogen content, urea-contaminated wastewater can be exploited as a renewable energy source. This hydrogen-rich wastewater is industrially produced in large amounts as a byproduct of fertilizer manufacturing plants and urine from humans and animals. Energy extraction from urea is environmentally required because it is considered an indirect treatment methodology. Urea is not a hazard material, but its predicted hydrolysis into ammonia gas results in required treatment of urea [1].

$$NH_2CONH_2 + H_2O \rightarrow 2NH_3 + CO_2 \quad (1)$$

In addition to gaseous pollution, there are two groups of bacteria (*Nitrobacter and Nitrosomonas*) that can create dangerous water pollution due to their ability to oxidize water-soluble ammonia into nitrate (NO_3^-) via an unstable intermediate nitrogen dioxide (NO_2) product [2]. This process occurs under anoxic conditions where several nitrous gases can be produced by the reduction of nitrate ions. In addition, ocean algae can be triggered by urea to produce a deadly toxin called domoic acid [3].

Economically, electricity generation from urea is the optimum strategy to extract the stored energy. In this regard, urea is exploited as an effective fuel in a direct urea fuel cell (DUFC). The corresponding theoretical cell potential is relatively high compared to that of some direct alcohol fuel cells according to the following reactions [4–7].

$$\text{Anode:} \quad CO(NH_2)_2 + 6OH^- \rightarrow N_2 + 5H_2O + CO_2 + 6e \qquad E^0 = -0.746\ V \quad (2)$$

$$\text{Cathode:} \quad 3H_2O + 1.5O_2 + 6e \rightarrow 6OH^- \qquad E^0 = +0.40\ V \quad (3)$$

$$\text{Overall:} \quad CO(NH_2)_2 + 1.5O_2 \rightarrow N_2 + 2H_2O + CO_2 \qquad E^0 = +1.146\ V \quad (4)$$

However, direct power generation from urea-polluted water requires an anode with a low onset potential (<0.4 V *vs.* NHE; the standard ORR potential in an alkaline medium). Unfortunately, developing a proper anode material with the required onset potential is not an easy task because the high overpotential of most reported materials (including precious metals) results in an onset potential over the threshold [8]. Therefore, researchers have tried to extract molecular hydrogen from urea by electrolysis according to the following reactions [9–11]:

$$\text{Anode:} \quad CO(NH_2)_2 + 6OH^- \rightarrow N_2 + 5H_2O + CO_2 + 6e \qquad E^0 = -0.746\ V \quad (5)$$

$$\text{Cathode:} \quad 6H_2O + 6e \rightarrow 3H_2 + 6OH^- \qquad E^0 = -0.829\ V \quad (6)$$

$$\text{Overall:} \quad CO(NH_2)_2 + H_2O \rightarrow N_2 + 3H_2 + CO_2 \qquad E^0 = -0.083\ V \quad (7)$$

Similar to DUFC, the observed small negative cell potential indicates an economical process; however, the real, very high anode overpotential of most proposed anode materials decreases the overall cell potential and consequently increases the electrical energy required for the oxidation process [8]. Therefore, research to develop a proper electrocatalyst with a high current density and low onset potential is ongoing.

Among the anode materials proposed for either DUFCs or urea electrolysis cells, nickel-based materials show the best performances [12–14]. However, their high onset potential (ca. 0.45 V *vs.* SHE) is a substantial constraint. Accordingly, trials have been conducted to overcome this dilemma. Modification of the morphology was proposed based on either synthesizing the catalyst in a specific nanostructural shape, including nickel nanowires [12], nickel nanoparticles [15], nickel-carbon sponges [16] and nickel nanoribbons [17], or exploiting the synergetic effect of other co-catalysts. Several elements have been utilized as co-catalysts in nickel-based anode materials, such as Mn [13], Co [9], N [18], and Zn [19]. Tin can form usefμ alloys with many metals, including Ni. In energy devices, the tin-nickel alloy electrode shows good performance in lithium-ion batteries [20,21]. To the best of our knowledge, this metal has not been investigated as a co-catalyst to enhance the electroactivity of nickel for urea oxidation. In addition to the aforementioned strategies, immobilization of a functional electrocatalyst on a proper support can result in a distinct positive impact on the electrocatalytic activity. Considering that electrooxidation reactions are theorized to be a combination of adsorption processes and chemical reactions, carbonaceous nanostructures have attracted attention as supports. Graphene, graphite, carbon nanotubes, and glassy carbon are the most widely used support materials [22–25]. Other researchers have tried other supports, such as mesoporous silica [26] and TiO_2 nanotubes [27], but due to their low adsorption capacity compared to that of carbonaceous materials, carbonaceous materials attract the most attention.

Among reported carbonaceous supports, nanofibers possess the lowest electron transfer resistance due to their large axial ratio. Typically, the large axial ratio of carbon nanofibers results in the elimination of the interfacial resistance that appears among particles in other morphologies [28]. The simplicity, high yield, low cost and applicability to different kinds of materials make electrospinning the most widely used nanofiber synthesis process in both industry and research [29–31].

In this study, tin was used as a novel co-catalyst, and a nanofibrous morphology was investigated to improve the electrocatalytic activity of nickel for urea oxidation. Typically, NiSn-incorporated carbon nanofibers were synthesized by calcination of electrospun nanofiber mats composed of nickel acetate tetrahydrate, tin chloride and poly(vinyl alcohol) under vacuum. Electrochemical measurements indicated that tin can strongly enhance the electrocatalytic activity of nickel; however, the co-catalyst content as well as the reaction temperature should be optimized. Interestingly, at 10 wt% and a high reaction temperature, the proposed electrode can be utilized as an anode in the DUFC.

Material and methods

Catalyst preparation

All the used chemicals were analytical grade and used without prior treatment. A 10 wt% aqueous solution of poly(vinyl alcohol) (PVA, Alfa Aesar, Seoul, South Korea) was prepared by adding polymer granules gradually to deionized (DI) water and stirring at 50 °C overnight. Then, nickel (II) acetate tetrahydrate (25 wt%; NiAc, Ni

$(CH_3COO)_2{\cdot}4H_2O$ Sigma Aldrich, Seoul, South Korea) and tin chloride ($SnCl_2$, Sigma Alrich, Seoul, South Korea) aqueous solutions were prepared. To make the electrospinning solution, a NiAc/PVA stock solution was first prepared by mixing PVA and NiAc solutions with a weight ratio of 3:1. The nickel acetate content in the final solution was maintained at ~5 wt%. Later, several $SnCl_2$-containing electrospinning solutions were prepared by adding the co-catalyst aqueous solution to 20 g of the NiAc/PVA solution. Electrospinning solutions containing 5, 10, 15, 25, and 35 wt% of $SnCl_2$ with respect to NiAc were prepared. The final solutions were stirred at 50 °C for 5 h. Preparation of the nanofibers was performed using a simple electrospinning device. The solution was placed in an inclined syringe to induce natural feeding. The process was carried out at a 20 kV DC potential with a 15 cm distance from the tip to the collector drum. Then, the nanofiber mats were dried under vacuum at 70 °C for 24 h. Finally, the mats were calcined at a heating rate of 2.5 deg/min under vacuum at different temperatures (700, 850, and 1000 °C) with a holding time of 3 h.

Characterization

The crystal structure of the prepared nanofibers was studied by X-ray diffraction analysis (XRD, Rigaku, Tokyo, Japan) with Cu Kα (λ = 1.540 Å) radiation over Bragg angles ranging from 20 to 80°. The nanofibrous morphology of the prepared electrocatalysts was checked by a scanning electron microscope (SEM, JEOL JSM-5900, Tokyo, Japan). The internal structure was investigated by studying the normal and high-resolution images that were obtained from a transmission electron microscope (JEOL JEM-2010, Tokyo, Japan). A VersaStat4 instrument (Princeton Applied Research, AMETEK scientific instruments, New York, USA) was used to measure the electrochemical characteristics. A simple 3-electrode cell with glassy carbon, Ag/AgCl and Pt electrodes as the working, reference and counter electrodes, respectively, was utilized as the reactor. The working electrode was prepared by deposition of the functional material on the active surface of a 3-mm glassy carbon electrode. Briefly, a suspension composed of 2 mg of the functional material, 20 μL of a Nafion solution (5 wt% in isopropanol) and 400 μL of isopropanol was sonicated for 0.5 h until a good dispersion was obtained. Then, a micropipette was used to deposit 5 μL of the suspension over the working electrode active area after cleaning and polishing the area. After natural drying, two additional drops were deposited by the same strategy. To study the kinetics of the electrooxidation reaction, electrochemical measurements were performed at different temperatures (12, 25, 35, 45 and 55 °C) by surrounding the cell with thermostated water. Electrochemical impedance sepectroscopy (EIS) measurments were carried out using VersaStat 4 instruemt (Princeton Applied Research, AMETEK scientific instruments, New York, USA) at the following coditions: Potential 0.6 V (*vs.* Ag/AgCl), start frequency 100,000 *Hz*, end frequency 0.01 *Hz*, amplitude 10 mV and points per decade 10.

Results and discussion

Electrocatalyst characterization

Catalyst morphology

Synthesis of inorganic nanofibers by the electrospinning process requires metallic precursors having a high polycondensation tendency to maintain a good nanofibrous morphology after the calcination process. In other words, with the proper polymer and optimization, the electrospinning parameters (e.g., applied voltage, tip-to-collector density, solution viscosity, relative humidity, etc.) guarantee the produced electrospun nanofibers have a good morphology. However, during the calcination process, the characteristics of the metallic precursor affect the final morphology. In this regard, metal alkoxides show the best performance as precursors for inorganic nanofiber synthesis by electrospinning [32]. Additionally, metal acetates could also be exploited as effective precursors due to their discovered polycondensation characteristic [33,34]. Fig. 1 shows the morphology of the nanofibers obtained after calcination at 700 °C with different tin chloride contents. Overall, the nanofibrous morphology was relatively constant for all formulations; however, the co-catalyst precursor content does have a strong impact on the morphology. As shown, nanoparticles formed along with the nanofibers with a corresponding density that depends on the content of $SnCl_2$ in the initial electrospun solution. Typically, with a low $SnCl_2$ content (up to 15 wt%; Fig. 1A–C), rare and well-distributed nanoparticles can be observed. However, when the co-catalyst content increased to 25 and 35 wt% (Fig. 1D and E, respectively), the number of nanoparticles dramatically increased. The largest nanoparticle size was obtained at the highest co-catalyst precursor content.

Increasing the calcination temperature to 850 °C did not change the morphology of the produced nanofibers, as displayed in Fig. 2. Typically, excluding 5 wt%, a low co-catalyst content maintained

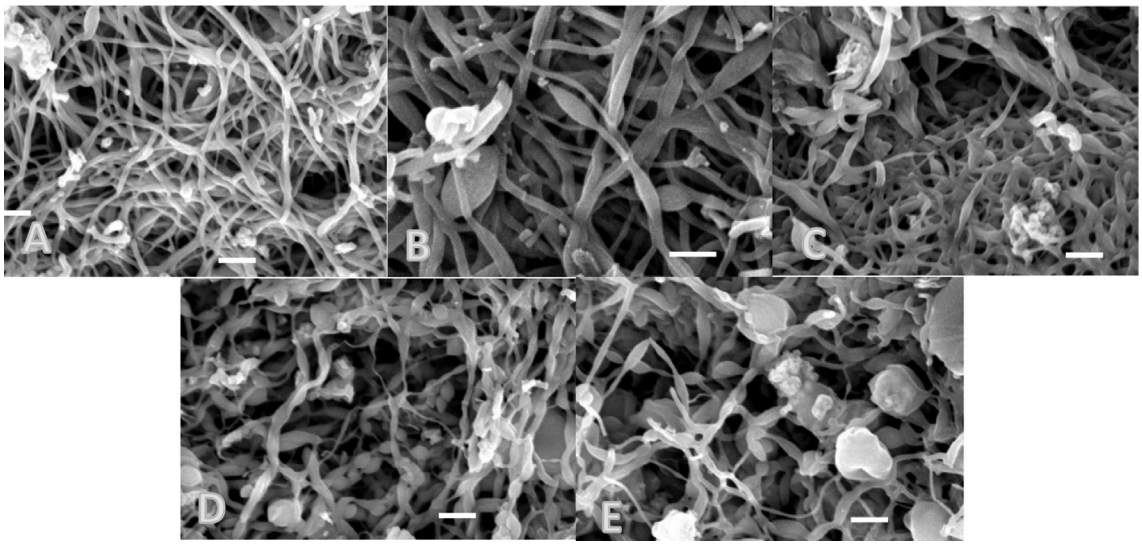

Fig. 1. Influence of $SnCl_2$ on the nanofibrous morphology after calcination of the electrospun mats at 700 °C: (A) 5%, (B) 10%, (C) 15%, (D) 25%, and (E) 35% $SnCl_2$. The scale bar is 1 μm.

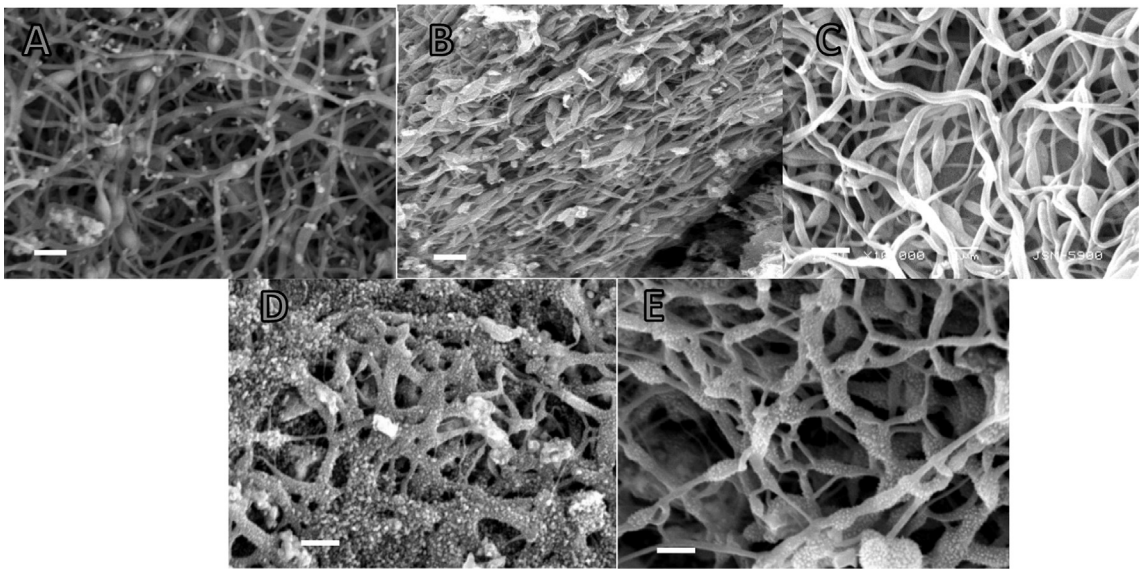

Fig. 2. Influence of $SnCl_2$ on the nanofibrous morphology after calcination of the electrospun mats at 850 °C: (A) 5%, (B) 10%, (C) 15%, (D) 25%, and (E) 35% $SnCl_2$. The scale bar is 1 μm.

the nanofibrous morphology, as shown in Fig. 2B and C. However, with a high concentration of $SnCl_2$ in the electrospun solution, the nanoparticles that formed were small compared to those observed at 700 °C. Additionally, increasing the calcination temperature leads to nanoparticles attaching to nanofibers. Notably, further increasing the calcination temperature to 1000 °C has a similar impact on the nanofibrous morphology. Briefly, with a co-catalyst content up to 15 wt%, almost no nanoparticles formed, while with high contents of co-catalyst in the electrospun solution, nanoparticles were observed; data are not shown. Fig. 3 shows a comparison of the morphologies of the nanofibers produced from an initial solution containing 10 wt% $SnCl_2$ and calcined at 700, 850, and 1000 °C.

Internal structure

The internal structure of the prepared nanofibers was investigated by transmission electron microscopy (TEM, Fig. 4). As shown in Fig. 4A, the prepared nanofibers are composed of crystalline nanoparticle-incorporated amorphous nanofibers. Fig. 4B and C display the Ni and Sn distributions along a selected line (the inset in Fig. 4A). The obtained data show that these two metals have similar distributions, which indicates the formation of alloy structures between the two metals. Moreover, these results indicate that the final product structure includes amorphous nanofibers surrounding crystalline nanoparticles composed mainly of nickel and tin.

Catalyst composition

X-ray diffraction analysis (XRD) is a reliable technique to investigate the composition of crystalline materials. Fig. 5 displays the patterns obtained for some nanofibers after calcination of the electrospun mats at 850 °C. As shown, the content of the tin precursor affects the composition of the produced metallic nanoparticles. Two forms of Ni/Sn alloy were detected for the nanofibers obtained from an electrospun solution with 5 wt% $SnCl_2$. The diffraction peaks at 2θ values of 28.6°, 39.3°, 42.5°, 44.8°, and 59.3°, corresponding to the (1 0 1), (2 0 0), (0 0 2), (2 0 1), and (2 0 2) crystal planes, respectively, indicate the formation of Ni_3Sn alloy (JCDPS# 35–1362), and the diffraction peaks at 2θ values of 30.7°, 34.8°, 43.5°, 44.6°, 55.1°, 57.6°, 59.8°, 63.9°, and 73.4° for the (1 0 1), (0 0 2), (1 0 2), (1 1 0), (2 0 1), (1 1 2), (1 0 3), (2 0 2), and (2 1 1) crystals planes, respectively, indicate the existence of a Ni_3Sn_2 alloy based on the JCDPS database (#06-0414). Increasing the co-catalyst content in the electrospun solution to 10 wt% leads to the formation of nanofibers with a single compound, Ni_3Sn_2. As shown, the standard peaks of Ni_3Sn_2 can be observed in the obtained pattern, and no peaks denoting the presence of other compounds were detected, indicating that these nanofibers are composed of a single NiSn chemical compound. For the other formulations, as shown in the figure, a Ni_3Sn and Ni_3Sn_2 mixture was also obtained. The formation of Ni/Sn alloys was also confirmed by the TEM results (Fig. 4). At $2\theta \sim 25°$, a wide peak was observed for all formulations, which corresponds to an experimental d spacing of 3.37 Å. The presence of

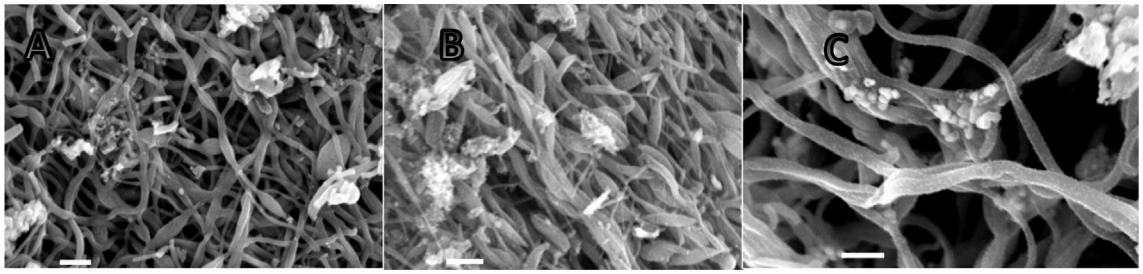

Fig. 3. Effect of the calcination temperature on the nanofibrous morphology of nanofibers obtained from electrospun mats with 10% $SnCl_2$: (A) 700, (B) 850. and (C) 1000 °C. The scale bar is 1 μm.

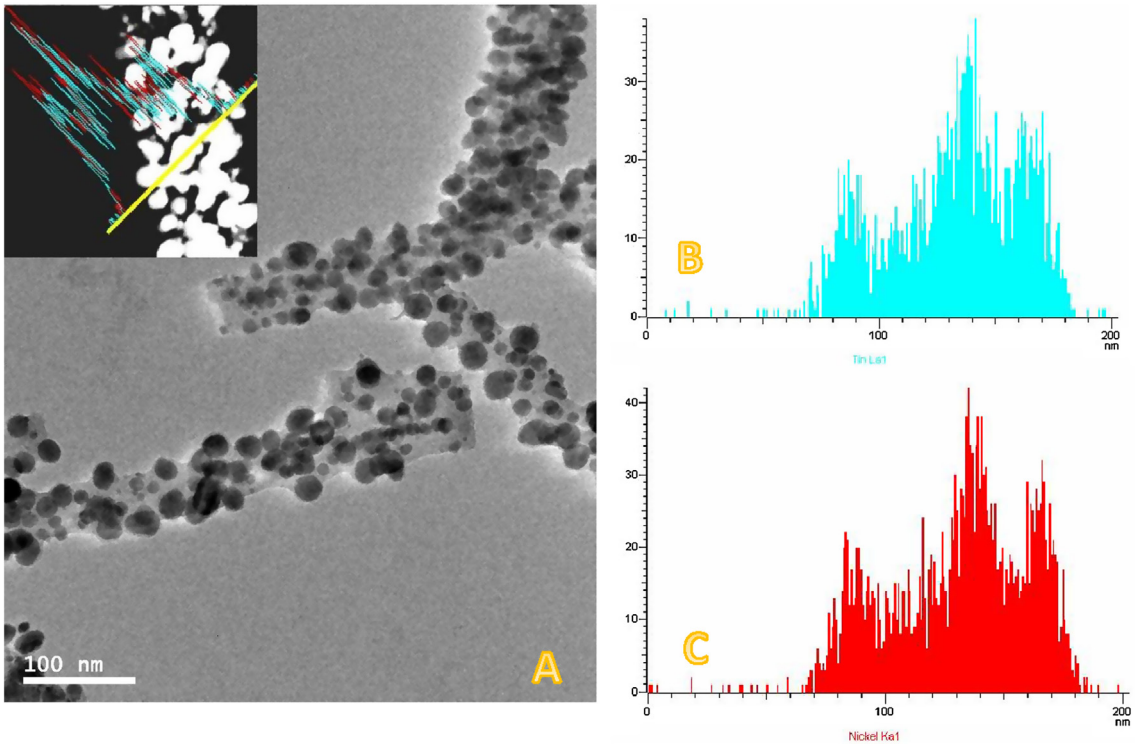

Fig. 4. (A) Normal TEM image of the prepared NiSn-incorporated CNFs (10 wt% sample) calcined at 850 °C. (B). and (C) Ni and Sn distributions along the selected line.

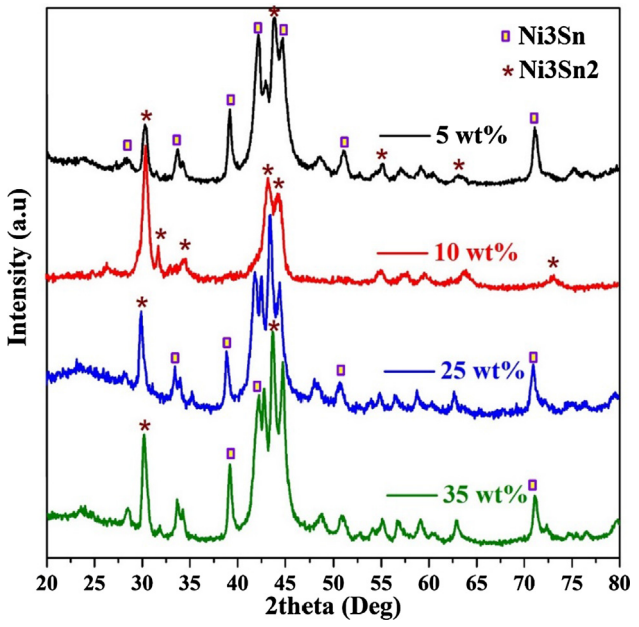

Fig. 5. XRD patterns of the nanofibers prepared at a calcination temperature of 850 °C.

this peak proves the formation of graphite-like carbon (*d* (0 0 2), JCPDS; 41-1487), and the peak can be assigned to the nanofiber matrix observed in the TEM results. Notably, a change in the calcination temperature did not strongly affect the produced nanofiber composition (data not shown). Overall, based on the results from the utilized characterization techniques, the prepared nanofibers are composed of NiSn alloy nanoparticle-incorporated amorphous graphite nanofibers. It is noteworthy mentioning that, formation of the bimetallic alloy with nickel can be considered the main reason behind imprisoning tin metal, which has low melting point (231 °C), in the final nanofiber product even at the utilized high calcination temperatures.

Electrochemical measurements

Influence of Sn addition

To properly investigate the efficacy of the selected co-catalyst in enhancing the electrocatalytic activity of nickel, Ni-incorporated nanofibers were prepared from a $SnCl_2$-free electrospun solution by the same procedure. Fig. 6A displays the electrocatalytic activity of Sn-free and 15 wt% Sn nanofibers (calcined at 700 °C) towards urea oxidation. The measurements were carried out using a 1.0 M urea solution (in 1.0 M KOH) at a scan rate of 0.05 V/s and reaction temperature of 30 °C. As shown, the addition of tin strongly enhances the electrocatalytic activity in terms of current density, and the maximum current density was increased almost 9-fold. The maximum current densities of the pristine and Sn-containing nanofibers are 9 and 77 mA/cm^2, respectively. Furthermore, increasing the calcination temperature to 850 °C improves the activities of both formulations, as shown in Fig. 6B. Moreover, the urea electrooxidation peak clearly appears for both samples. However, the upward slope of the curves indicates that the calcination temperature has a stronger impact on the pristine nickel-incorporated carbon nanofibers than the Sn-containing ones. In detail, the current density increases from 9 to 17 mA/cm^2 (~90% increase) and from 77 to 81 mA/cm^2 (~5% increase) for the pristine and alloy nanoparticle-incorporated nanofibers, respectively.

Although the obtained results are interesting due to the potent increase in the electrocatalytic activity of nickel in terms of the amount of urea oxidized on the surface of the proposed catalyst, this finding is limited to urea electrolysis cells. According to these data, inserting Sn as a co-catalyst with nickel could successfully accelerate the oxidation reaction but does not change the required activation energy. As shown in the figure, almost no improvement in the onset potential was achieved at this co-catalyst content;

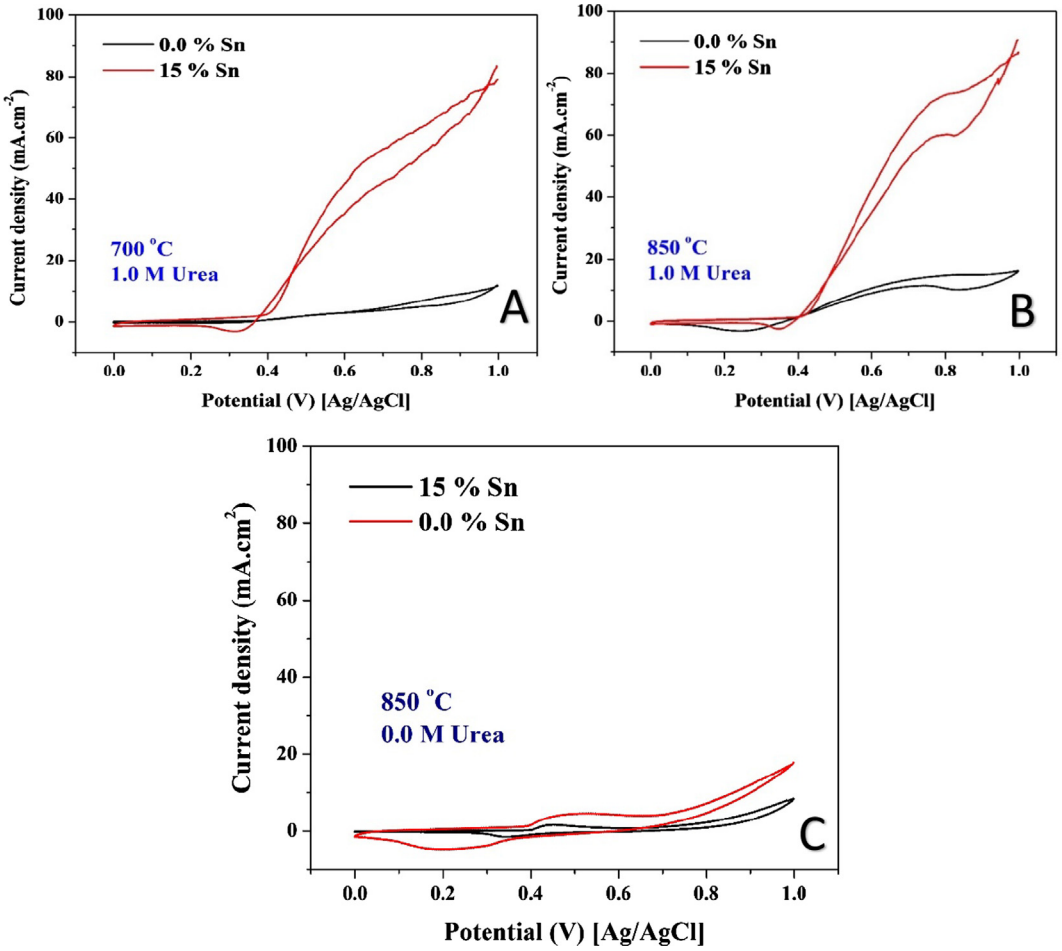

Fig. 6. Influence of Sn addition (15 wt%) on the electrocatalytic activity of the proposed NiSn-incorporated carbon nanofibers calcined at 700 °C (A) and 850 °C (B) for oxidation of a 1.0 M urea solution in 1.0 M KOH at 30 °C with a 50 mV/s scan rate. Panel C displays the activity of pristine nickel and NiSn (15 wt%) nanoparticles-incorporated CNFs in urea-free 1.0 KOH solution.

both samples are not useable as anodes in DUFCs. Panel C demonstrates the CV measurements for the pristine nickel and NiSn (15 wt%) nanoparticles-incorporated carbon nanofibers calcined at 850 °C in presence of urea-free 1.0 KOH solution. The results confirm the electrocatalytic activity of the proposed nanofibers toward urea electrooxidation. As shown, absence of urea results in a dramatic decrease in the observed current density compared to urea-containing solutions (Fig. 6A and B). It is noteworthy mentioning that the nanofibers prepared at other calcination temperatures (i.e. 700 and 1000 °C) showed almost similar results.

Influence of Sn content

The synergetic effect of tin in the proposed NiSn-incorporated carbon nanofibers was studied by investigating the electrocatalytic activity of the nanofibers with different Sn contents. As shown in Fig. 7A, changing the Sn content in the proposed electrocatalyst

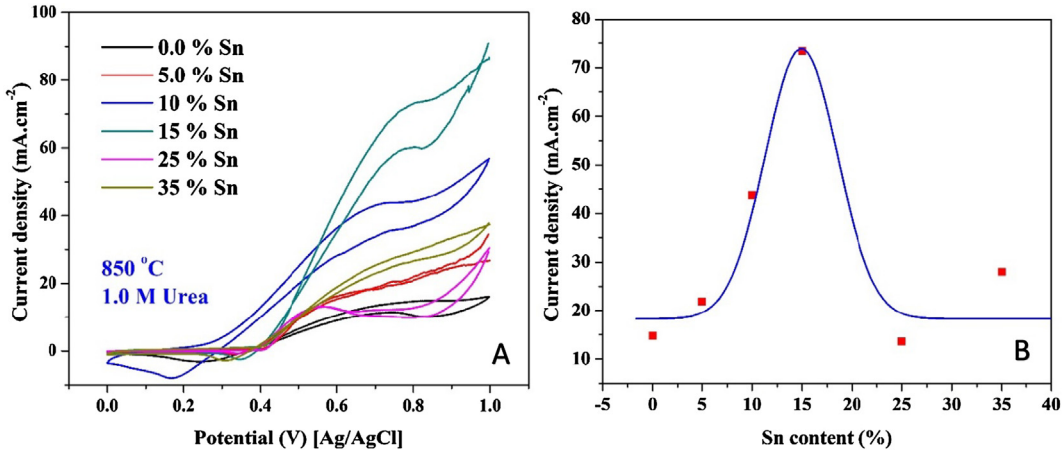

Fig. 7. (A) Influence of Sn content on the electrocatalytic activity of the proposed NiSn-incorporated carbon nanofibers calcined at 850 °C for the oxidation of a 1.0 M urea solution in 1.0 M KOH at 30 °C with a 50 mV/s scan rate. (B) The relationship between Sn content and the anodic peak current density.

has a strong impact on the electrocatalytic activity. Fig. 7B displays the relationship between the $SnCl_2$ content in the electrospun solution and the maximum current density of the oxidation peak. For the investigated contents, a Gaussian shape was obtained with a peak at 15 wt%. Gaussian curve was selected as the best model to fit the data points by the utilized software (Origin 8.1). In addition to optimizing the tin content to maximize the current density, Fig. 7A shows that the onset potential can also be improved by this effective co-catalyst. The onset potential decreased to 195 mV (*vs.* Ag/AgCl) for the nanofibers containing 10 wt%, and all other formulations had an onset potential of ~415 mV. The last finding is very important as the proposed nanofibers can be exploited as an anode material in DUFCs.

From a kinetic point of view, most electrochemical reactions are non-elementary. In other words, the reactions proceed in multiple steps with one (or more) rate controlling step(s). Compared to methanol and ethanol oxidation reactions, whose kinetics have been intensively studied [35,36], to the best of our knowledge, the kinetics of urea oxidation have not been studied to determine the reaction mechanism and rate controlling step(s). However, the urea oxidation process is believed to be a non-elementary reaction, especially because urea has a higher molecular weight than methanol [37].

In heterogeneous catalytic reactions, an effective catalyst can directly enhance the reaction rate by decreasing the activation energy. Moreover, a heterogeneous catalyst can indirectly accelerate a reaction by improving the reaction mechanism, e.g., decreasing the number of reaction steps, minimizing the number of rate controlling steps, etc. Based on the aforementioned hypotheses, the Sn-containing nanofibers, excluding the 10 wt% sample, could indirectly enhance the urea oxidation reaction. In detail, the compositions of the NiSn nanoparticles created from these formulations may not decrease the required activation energy, but they might improve the oxidation pathway to overcome a very slow step(s) occurring on the surface of pristine nickel and/or accelerate the adsorption of urea (or intermediates), which consequently improve the overall process. In this regard, the nanofibers prepared from an electrospinning solution with 15 wt% $SnCl_2$ had the optimum composition.

On the other hand, the 10 wt% sample, which is composed of a single NiSn alloy, could directly improve the oxidation process by decreasing the activation energy, as reflected by the large decrease in the onset potential.

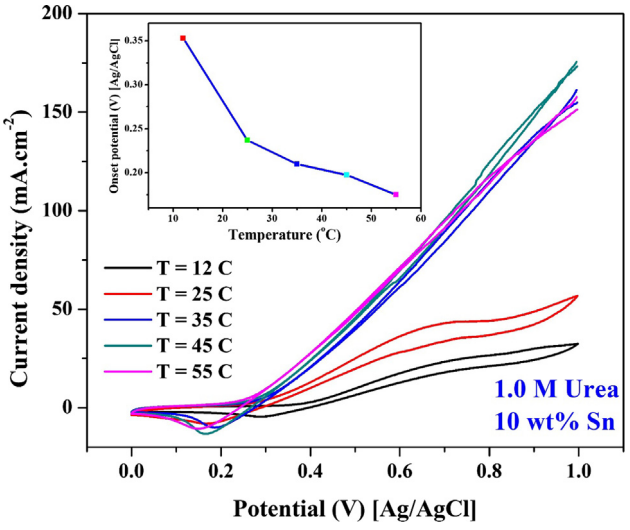

Fig. 8. Influence of the electrooxidation temperature of urea (1.0 M in 1.0 KOH) over the surface of NiSn-incorporated carbon nanofibers prepared from a solution containing 10 wt% $SnCl_2$ and calcined at 850 °C at 50 mV/s. The inset displays the effect of the reaction temperature on the onset potential.

Fig. 8 displays the influence of the reaction temperature on the electrocatalytic activity of the 10 wt% nanofibers. As shown in the figure, the reaction temperature had a very strong impact on the generated current density, which indicated the oxidation of urea molecules over the surface of these nanofibers is rapid. The maximum current density reached ~175 mA/cm^2 at high temperatures (above 35 °C). Furthermore, as shown in the associated inset, the onset potential of the reaction is inversely related to the temperature. Based on this result, the proposed nanofibers can be exploited as anode materials in DUFCs at cell temperatures above 50 °C. Numerically, the onset potential decreased from 353 mV at 12 °C to 175 mV (*vs.* Ag/AgCl) at 55 °C.

The results obtained in Fig. 8 provide evidence that the urea oxidation process is a non-elementary reaction. If the reaction is elementary, the data should satisfy the Arrhenius equation. In other words, an increase in the temperature should enhance the current density (i.e., increase the rate of reaction). However, as shown in the figure, almost no observable change in the reaction rate could be detected at high temperatures. Additionally, for a single-step elementary reaction, the activation energy is not a variable in the Arrhenius equation; the variables are the reaction constant and temperature [38]. Therefore, if urea oxidation is an elementary reaction, the onset potential has to be independent of the temperature. Overall, the obtained results indicate that this DUFC-applicable sample can enhance the activation energy of the rate controlling steps in the multistep urea reaction.

Influence of urea concentration

Due to mass transfer limitations, the urea concentration has to be optimized. From a kinetic point of view, the reactant concentration has a distinct influence on the rate of the reaction until the catalyst surface is completely covered. After the catalyst surface is covered, increasing the concentration does not impact the performance and reaction rate. Therefore, many heterogeneous catalytic reactions are considered zero-order reactions. Fig. 9 displays the influence of the urea concentration on the observed current density with the nanofibers that provided the maximum current density. As shown in Fig. 9A, for the nanofibers prepared from calcination of electrospun mats containing 15 wt% $SnCl_2$ at 700 °C, the maximum current density is associated with urea concentrations of 0.33 and 1.0 M. Above those concentrations, further increasing the concentration results in a slight decrease in the reaction rate. These results indicate urea oxidation is a zero-order reaction and simultaneously validate the aforementioned hypothesis.

Increasing the calcination temperature to 850 °C leads to a distinct improvement in the crystallinity of the nanofibers, which was reflected by the distinguished performance compared to that of the electrocatalyst prepared at 700 °C, as shown in Fig. 9B. Briefly, the urea oxidation process became a concentration-dependent reaction. As shown in the figure, the generated current substantially changes with a change in the concentration of the urea solution. The maximum current density was 17.8, 73.6, and 88.4 mA/cm^2 for urea concentrations of 0.33, 1.0 and 2.0 M, respectively. For 3.0 M urea, the current density decreased to 73.5 mA/cm^2. These results indicate that for nanofibers prepared at a low calcination temperature, the urea oxidation process is not controlled by mass transfer. Thus, the activity is relatively low, and the surface can be covered by the reactant and/or intermediate molecules at a low concentration. However, due to the higher activity created upon increasing the calcination temperature to 850 °C, the oxidation rate improves. Therefore, increasing the concentration enhances the generated current density up to a certain concentration (2.0 M). Above this concentration, the active surface will be covered by urea molecules.

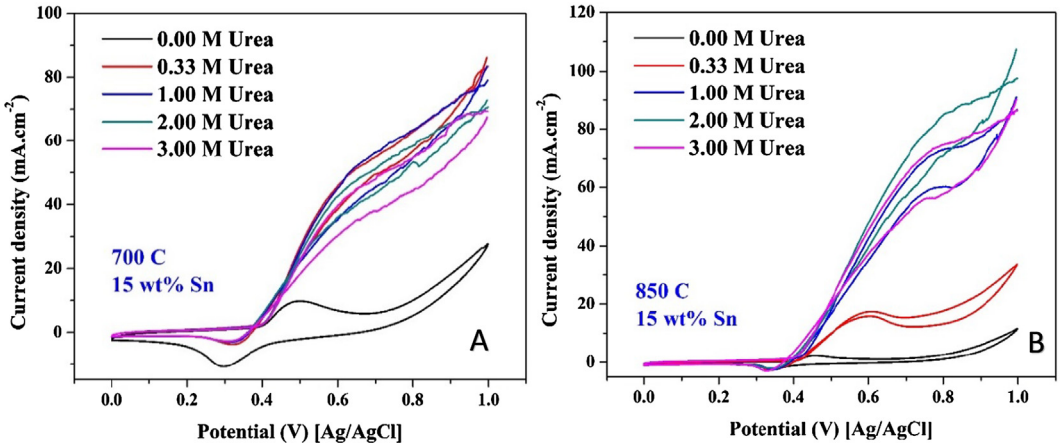

Fig. 9. Influence of the urea concentration on the electrocatalytic activity of NiSn-incorporated carbon nanofibers prepared from an electrospinning solution with 15 wt% $SnCl_2$ and calcined at 700 °C (A) and 850 °C (B) at 30 °C with a scan rate 50 mV/s.

Influence of calcination temperature

As shown in the previous results, the nanofibers prepared at 850 °C exhibited a better performance than those synthesized at 700 °C. Therefore, to properly optimize the calcination temperature, electrochemical measurements were performed using nanofibers with a similar tin content (10 wt%) that were sintered at different temperatures: 700, 850, and 1000 °C. As shown in Fig. 10, the nanofibers prepared at 850 °C have the best performance at all urea concentrations.

Based on the XRD results, the change in the composition with a change in the calcination temperature is trivial. Therefore, to understand how the calcination temperature affects the electrocatalytic activity, thermal gravimetric analysis was carried out (Fig. 11). As shown in Fig. 11A, there is a low-weight decrease that matches a small peak at ~95 °C in the first derivative plot for the obtained data (Fig. 11B). This weight loss can be attributed to the evaporation of physical moisture. Later, a sharp decrease in weight, which is shown as a high-intensity peak in Fig. 11B, can be

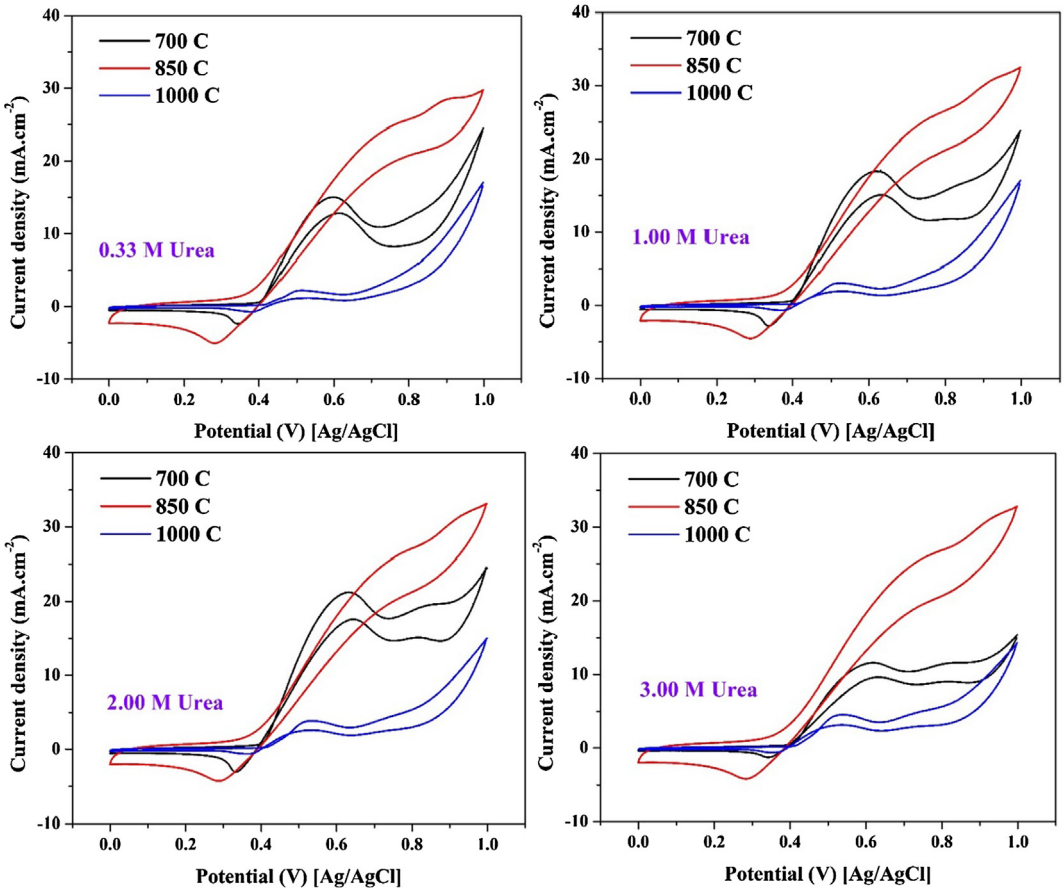

Fig. 10. Effect of the calcination temperature on the electrocatalytic activity of the proposed NiSn-incorporated carbon nanofibers prepared from a solution containing 10 wt% $SnCl_2$ at different urea concentrations with a reaction temperature of 12 °C and scan rate of 50 mV/s.

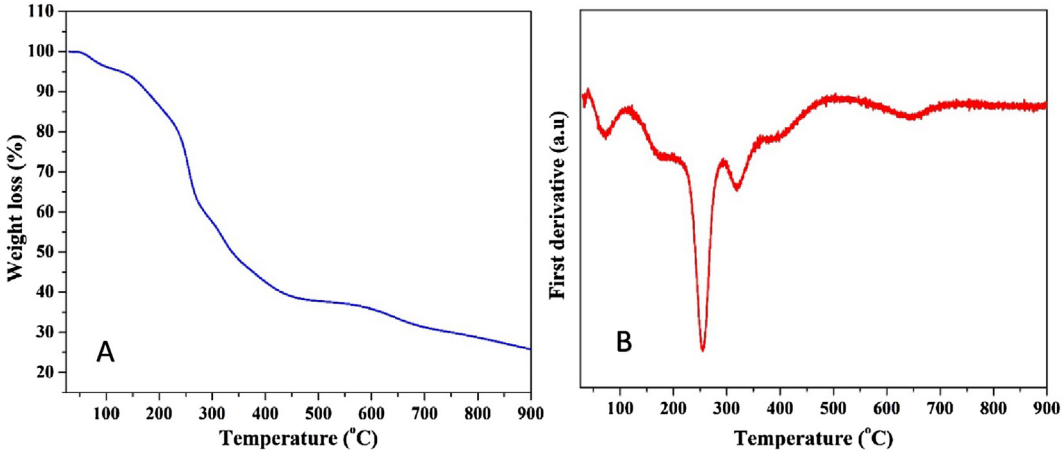

Fig. 11. Thermal gravimetric analysis of the nanofibers prepared from an electrospinning solution containing 10 wt% $SnCl_2$ (A) and the first derivative of the obtained data (B).

observed. This weight-loss peak can be assigned to the decomposition of the utilized polymer. The remaining peaks represent the decomposition of nickel acetate to form pristine nickel according the following equations [14,39,40].

$$Ni(CH_3COO)_2{\cdot}4H_2O \rightarrow 0.86Ni(CH_3COO)_2{\cdot}0.14Ni(OH)_2 + 0.28CH_3COOH + 3.72H_2O \quad (8)$$

$$0.86\ Ni(CH_3COO)_2{\cdot}0.14Ni(OH)_2 \rightarrow NiCO_3 + NiO + CH_3COCH_3 + H_2O \quad (9)$$

$$NiCO_3 \rightarrow NiO + CO_2 \quad (10)$$

$$NiO + CO \rightarrow Ni + CO_2 \quad (11)$$

Complete reduction of tin chloride was achieved due to the formation of strong reducing gases (CO and H_2) from the decomposition of acetate ions.

Importantly, the absence of any peak in Fig. 11B above ~650 °C can be explained as a small gradual weight loss that was not due to a chemical reaction. This small weight decrease (above 650 °C) can also be observed in Fig. 11A. The XRD results (Fig. 4) indicated that this sample was composed of a single metallic compound (Ni_3Sn_2) and graphite. Considering the high melting point of the metallic nanoparticles, the observed weight loss can be assigned to the carbonaceous counterpart, indicating that the graphite layer gradually decreased with increasing temperature. As explained in the introduction section, the carbon support plays an important role in electrooxidation processes because of its adsorption capacity. Accordingly, the very low observed performance of the nanofibers prepared at 1000 °C is due to the low graphite content of the proposed electrocatalyst.

Catalyst stability

The stability of the transition metal-based electrocatalysts is usually uncertain. Fig. 12 displays the chronoamperometry analysis of the nanofibers with the lowest onset potential at 12 °C. The measurement was carried out by applying multistep potential. Typically, the applied potential was increased 0.1 V every 500 s within the potential window from 0.3 to 1.0 V (*vs.* Ag/AgCl). As shown in Fig. 12, especially at low applied potentials (<0.8 V), a very good stability was observed. These results indicate additional advantages for exploiting tin as a co-catalyst to enhance the electrocatalytic activity of nickel materials for urea oxidation.

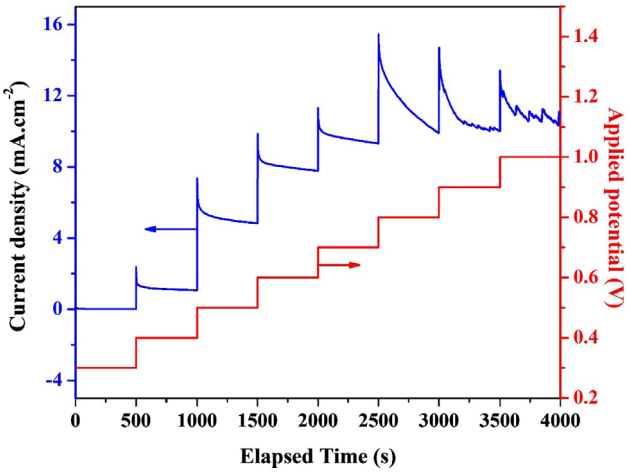

Fig. 12. Chronoamperometry analysis at various potentials for NiSn-incorporated carbon nanofibers prepared from a sol-gel solution containing 10 wt% $SnCl_2$ and calcined at 850 °C.

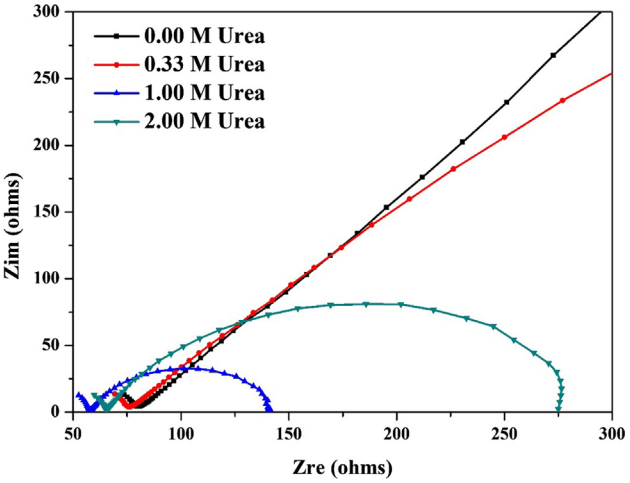

Fig. 13. Nyquist plots for different concentrations of urea oxidation reaction at 0.6 V [*vs.* Ag/AgCl] on the surface of the proposed electrode (10 wt%) calcined at 850 °C.

Electrochemical impedance sepectroscopy (EIS)

EIS is a useful method for studying the interfacial properties of the electro catalyst [41]. The impedance is the summation of real, Z_{re}, and imaginary, Z_{im}, components contributed by the resistance and capacitance of the cell [42]. In this study EIS was employed to investigate electrocatalytic activity of the proposed electrode. EIS measurements at different urea solution concentrations were performed at 0.6 V (*vs.* Ag/AgCl). Nyquist plots for the utilized samples are displayed in Fig. 13. In the Nyquist plot, the Faradaic reaction (urea oxidation) is usually displayed by capacitive loop with a diameter almost matching the charge transfer resistance (R_{CT}). As shown in the figure, the urea-free solution did not show a Faradaic reaction. On the other hand, as shown in this figure, the capacitive loops appear with increasing the urea concentration which clearly indicates the electrocatalytic activity of the proposed electrode. However, the smallest charge transfer resistance is corresponding to 2.0 urea solution. It is noteworthy mentioning that low charge transfer resistance demonstrates fast electron-transfer rate on the electrocatalyst [43].

Conclusions

NiSn bimetallic alloy nanoparticle-incorporated carbon nanofibers can be obtained from calcination of electrospun mats composed of nickel acetate, tin chloride and poly(vinyl alcohol) under vacuum. The addition of a tin precursor to the electrospinning solution results in the formation of nanoparticles along with the prepared NiSn/carbon nanofiber composite, especially at high contents (more than 15 wt%). The calcination temperature has almost no impact on the bimetallic nanoparticle composition; however, increasing the calcination temperature leads to a decrease in the graphite content, which negatively affects the electrocatalytic activity of the catalyst for urea oxidation. The proposed electrocatalyst can be utilized effectively in urea electrolysis cells when the co-catalyst content and calcination temperature are 15 wt% and 850 °C, respectively. However, to be exploited in DUFCs, the co-catalyst content in the initial electrospun solution must be 10 wt%. The proposed catalyst shows very good stability, especially at low applied potentials.

Conflict of interest

The authors have declared no conflict of interest.

Compliance with Ethics Requirements

This article does not contain any studies with human or animal subjects.

Acknowledgement

The authors would like to extend their thanks to The Deanship of Scientific Research King Saud University, Riyadh, Saudi Arabia for their support of this work through the group RG-1439-042.

References

[1] Kojima S, Bohner A, Von Wirén N. Molecular mechanisms of urea transport in plants. J Membr biol 2006;212:83–91.
[2] Ongley ED. Control of water pollution from agriculture. Food Agric Org 1996.
[3] Bargu S, Silver MW, Ohman MD, Benitez-Nelson CR, Garrison DL. Mystery behind Hitchcock's birds. Nat Geosci 2012;5:2–3.
[4] Lan R, Tao S, Irvine JT. A direct urea fuel cell–power from fertiliser and waste. Energy Environ Sci 2010;3:438–41.
[5] Xu W, Zhang H, Li G, Wu Z. Nickel-cobalt bimetallic anode catalysts for direct urea fuel cell. Sci Rep 2014;4:5863.
[6] Yousef A, El-Newehy MH, Al-Deyab SS, Barakat NA. Facile synthesis of Ni-decorated multi-layers graphene sheets as effective anode for direct urea fuel cells. Arab J Chem 2017;10:811–22.
[7] Barakat N, Alajami M, Ghouri ZK, Al-Meer S. CoNi nanoparticles/CNT composite as effective anode for direct urea fuel cells. Int J Electrochem Sci 2018;13:4693–9.
[8] Barakat NA, Alajami M, Al Haj Y, Obaid M, Al-Meer S. Enhanced onset potential NiMn-decorated activated carbon as effective and applicable anode in urea fuel cells. Catal Commun 2017;97:32–6.
[9] Yan W, Wang D, Botte GG. Nickel and cobalt bimetallic hydroxide catalysts for urea electro-oxidation. Electrochim Acta 2012;61:25–30.
[10] King RL, Botte GG. Investigation of multi-metal catalysts for stable hydrogen production via urea electrolysis. J Power Sources 2011;196:9579–84.
[11] Wang D, Yan W, Vijapur SH, Botte GG. Electrochemically reduced graphene oxide–nickel nanocomposites for urea electrolysis. Electrochim Acta 2013;89:732–6.
[12] Guo F, Ye K, Cheng K, Wang G, Cao D. Preparation of nickel nanowire arrays electrode for urea electro-oxidation in alkaline medium. J Power Sources 2015;278:562–8.
[13] Barakat NA, El-Newehy MH, Yasin AS, Ghouri ZK, Al-Deyab SS. Ni&Mn nanoparticles-decorated carbon nanofibers as effective electrocatalyst for urea oxidation. Appl Catal A: General 2016;510:180–8.
[14] Barakat NA, Motlak M, Ghouri ZK, Yasin AS, El-Newehy MH, Al-Deyab SS. Nickel nanoparticles-decorated graphene as highly effective and stable electrocatalyst for urea electrooxidation. J Mol Catal A: Chem 2016;421:83–91.
[15] Vedharathinam V, Botte GG. Understanding the electro-catalytic oxidation mechanism of urea on nickel electrodes in alkaline medium. Electrochim Acta 2012;81:292–300.
[16] Ye K, Zhang D, Guo F, Cheng K, Wang G, Cao D. Highly porous nickel@ carbon sponge as a novel type of three-dimensional anode with low cost for high catalytic performance of urea electro-oxidation in alkaline medium. J Power Sources 2015;283:408–15.
[17] Wang D, Yan W, Vijapur SH, Botte GG. Enhanced electrocatalytic oxidation of urea based on nickel hydroxide nanoribbons. J Power Sources 2012;217:498–502.
[18] Barakat NA, Yassin MA, Yasin AS, Al-Meer S. Influence of nitrogen doping on the electrocatalytic activity of Ni-incorporated carbon nanofibers toward urea oxidation. Int J Hydrogen Energy. 2017;42:21741–50.
[19] Yan W, Wang D, Botte GG. Electrochemical decomposition of urea with Ni-based catalysts. Appl Catal B-Environ 2012;127:221–6.
[20] Jiang D, Ma X, Fu Y. High-performance Sn–Ni alloy nanorod electrodes prepared by electrodeposition for lithium ion rechargeable batteries. J Appl Electrochem 2012;42:555–9.
[21] Mukaibo H, Momma T, Osaka T. Changes of electro-deposited Sn–Ni alloy thin film for lithium ion battery anodes during charge discharge cycling. J Power Sources 2005;146:457–63.
[22] Zhao Y, Yang X, Tian J, Wang F, Zhan L. Methanol electro-oxidation on Ni@ Pd core-shell nanoparticles supported on multi-walled carbon nanotubes in alkaline media. Int J Hydrogen Energy 2010;35:3249–57.
[23] Asgari M, Maragheh MG, Davarkhah R, Lohrasbi E, Golikand AN. Electrocatalytic oxidation of methanol on the nickel–cobalt modified glassy carbon electrode in alkaline medium. Electrochim Acta 2012;59:284–9.
[24] Zhong J-P, Fan Y-J, Wang H, Wang R-X, Fan L-L, Shen X-C, et al. Highly active Pt nanoparticles on nickel phthalocyanine functionalized graphene nanosheets for methanol electrooxidation. Electrochim Acta 2013;113:653–60.
[25] Yu M, Chen J, Liu J, Li S, Ma Y, Zhang J, et al. Mesoporous NiCo2O4 nanoneedles grown on 3D graphene-nickel foam for supercapacitor and methanol electro-oxidation. Electrochim Acta 2015;151:99–108.
[26] Azizi SN, Ghasemi S, Chiani E. Nickel/mesoporous silica (SBA-15) modified electrode: an effective porous material for electrooxidation of methanol. Electrochim Acta 2013;88:463–72.
[27] Hosseini M, Momeni M, Faraji M. Highly active nickel nanoparticles supported on TiO2 nanotube electrodes for methanol electrooxidation. Electroanalysis 2010;22:2620–5.
[28] Barakat NA, Abdelkareem MA, El-Newehy M, Kim HY. Influence of the nanofibrous morphology on the catalytic activity of NiO nanostructures: an effective impact toward methanol electrooxidation. Nanoscale Res Lett 2013;8:402.
[29] Barakat NA, Kanjwal MA, Chronakis IS, Kim HY. Influence of temperature on the photodegradation process using Ag-doped TiO2 nanostructures: negative impact with the nanofibers. J Mol Catal A: Chem 2013;366:333–40.
[30] Barakat NA, Motlak M, Kim B-S, El-Deen AG, Al-Deyab SS, Hamza A. Carbon nanofibers doped by NixCo1 – x alloy nanoparticles as effective and stable non precious electrocatalyst for methanol oxidation in alkaline media. J Mol Catal A: Chem 2014;394:177–87.
[31] Yousef A, Brooks RM, Abdelkareem MA, Khamaj JA, El-Halwany M, Barakat NA, et al. Electrospun NiCu nanoalloy decorated on carbon nanofibers as chemical stable electrocatalyst for methanol oxidation. ECS Electrochem Lett 2015;4:F51–5.
[32] Maneeratana V, Sigmund WM. Continuous hollow alumina gel fibers by direct electrospinning of an alkoxide-based precursor. Chem Eng J 2008;137:137–43.
[33] Yang X, Shao C, Guan H, Li X, Gong J. Preparation and characterization of ZnO nanofibers by using electrospun PVA/zinc acetate composite fiber as precursor. Inorg Chem Commun 2004;7:176–8.
[34] Yousef A, Barakat NA, Amna T, Unnithan AR, Al-Deyab SS, Kim HY. Influence of CdO-doping on the photoluminescence properties of ZnO nanofibers: effective

visible light photocatalyst for waste water treatment. J Lumin 2012;132:1668–77.
[35] Vigier F, Coutanceau C, Hahn F, Belgsir E, Lamy C. On the mechanism of ethanol electro-oxidation on Pt and PtSn catalysts: electrochemical and in situ IR reflectance spectroscopy studies. J Electroanal Chem 2004;563:81–9.
[36] Tripković A, Popović KD, Grgur B, Blizanac B, Ross P, Marković N. Methanol electrooxidation on supported Pt and PtRu catalysts in acid and alkaline solutions. Electrochim Acta 2002;47:3707–14.
[37] Herrero E, Chrzanowski W, Wieckowski A. Dual path mechanism in methanol electrooxidation on a platinum electrode. J Phys Chem 1995;99:10423–4.
[38] Taghizade Firozjaee T, Mehrdadi N, Baghdadi M, Nabi Bidhendi G. Application of nanotechnology in pesticides removal from aqueous solutions - a review. Int J Nanosci Nanotechnol 2018;14:43–56.
[39] De Jesus JC, González I, Quevedo A, Puerta T. Thermal decomposition of nickel acetate tetrahydrate: an integrated study by TGA, QMS and XPS techniques. J Mol Catal A: Chem 2005;228:283–91.
[40] Barakat NA, Khalil KA, Mahmoud IH, Kanjwal MA, Sheikh FA, Kim HY. CoNi bimetallic nanofibers by electrospinning: nickel-based soft magnetic material with improved magnetic properties. J Phys Chem C 2010;114:15589–93.
[41] Parsa A, Amanzadeh-Salout S. Electrocatalytic activity and electrochemical impedance spectroscopy of poly (aniline-co-ortho-phenylenediamine) modified electrode on ascorbic acid. Orient J Chem 2016;32:2051–8.
[42] Feng L-J, Zhang X-H, Zhao D-M, Wang S-F. Electrochemical studies of bovine serum albumin immobilization onto the poly-o-phenylenediamine and carbon-coated nickel composite film and its interaction with papaverine. Sensors Actuators B: Chem 2011;152:88–93.
[43] Döner A, Telli E, Kardaş G. Electrocatalysis of Ni-promoted Cd coated graphite toward methanol oxidation in alkaline medium. J Power Sources 2012;205:71–9.